Hepatitis C virus replication in mice with chimeric human livers

DAVID F. MERCER[1], DANIEL E. SCHILLER[1], JOHN F. ELLIOTT[2], DONNA N. DOUGLAS[1], CHUNHAI HAO[3], ALINE RINFRET[4], WILLIAM R. ADDISON[2], KARL P. FISCHER[2], THOMAS A. CHURCHILL[1], JONATHAN R.T. LAKEY[1], DAVID L.J. TYRRELL[2] & NORMAN M. KNETEMAN[1]

[1]*Surgical-Medical Research Institute, Department of Surgery,* [2]*Department of Medical Microbiology and Immunology and* [3]*Department of Pathology, University of Alberta, Edmonton, Alberta, Canada*
[4]*Centre de Recherche du CHUM, Hôpital Saint-Luc, Montréal, Québec, Canada*
Correspondence should be addressed to N.M.K.; email: nknetema@cha.ab.ca

Lack of a small animal model of the human hepatitis C virus (HCV) has impeded development of antiviral therapies against this epidemic infection. By transplanting normal human hepatocytes into SCID mice carrying a plasminogen activator transgene (*Alb-uPA*), we generated mice with chimeric human livers. Homozygosity of *Alb-uPA* was associated with significantly higher levels of human hepatocyte engraftment, and these mice developed prolonged HCV infections with high viral titers after inoculation with infected human serum. Initial increases in total viral load were up to 1950-fold, with replication confirmed by detection of negative-strand viral RNA in transplanted livers. HCV viral proteins were localized to human hepatocyte nodules, and infection was serially passaged through three generations of mice confirming both synthesis and release of infectious viral particles. These chimeric mice represent the first murine model suitable for studying the human hepatitis C virus *in vivo*.

Human liver disease caused by the hepatitis C virus has emerged as a major challenge to the medical community, affecting an estimated 175 million people worldwide[1]. Elucidation of the viral sequence in 1989 (ref. 2) initiated concerted study of HCV. Antiviral therapy with combination interferon and ribavirin is effective in selected patients, but many do not respond or tolerate therapy poorly, underscoring a need for improvement. Development of effective therapeutic strategies has been significantly hampered by difficulties in establishing *in vitro* and *in vivo* models of viral replication.

The *Alb-uPA* transgenic mouse, developed in 1990 to study neonatal bleeding disorders[3], carries a tandem array of four murine urokinase genes controlled by an albumin promoter. This transgene targets urokinase over-production to the liver resulting in a profoundly hypofibrinogenemic state and accelerated hepatocyte death. Through random somatic mutations, individual hepatocytes spontaneously delete portions of the transgene array, providing a significant replicative advantage over surrounding cells, and resulting in repopulation of the liver with largely nontransgenic cells[4]. This survival advantage is extended to hepatocytes transplanted from mouse, rat[5] and woodchuck donors[6], and recently in hepadnavirus systems using immortalized[7] and nonimmortalized[8] human hepatocytes.

Human graft survival correlates with *Alb-uPA* zygosity

We crossed *Alb-uPA* and C.b-17/SCID/*bg* mouse lines, and through selective backcrosses bred the SCID trait to homozygosity. In initial experiments, homozygous SCID animals carrying the *Alb-uPA* transgene in hemizygous fashion were crossed, and litters were transplanted with freshly isolated human hepatocytes. Human albumin, produced exclusively by human hepatocytes, was used as an indicator of graft function[9].

In a pilot study of 36 transplants, strong human-albumin signals at 4–5 weeks post-transplant were demonstrated in the serum of 19 recipients. We detected human-albumin bands at 2 weeks post-transplant which increased in intensity over 4–6-week time points, indicating graft expansion (Fig. 1*a*). Blinded genotype analysis revealed that all strongly human-albumin–positive animals carried *Alb-uPA*, whereas the remainder did not.

Despite initially strong human-albumin signals, some recipients showed extinction of signal around 14 weeks, whereas a second subset maintained strong signals beyond 30 weeks (Fig. 1*b*). As these graft recipients were progeny of heterozygous crosses, we hypothesized this divergence was the result of zygosity of *Alb-uPA*. Transgenic and endogenous *uPA* were distinguishable by Southern-blot analysis, with the signal ratio then used to determine the zygosity of the transgene array (Fig. 1*c*). Genomic DNA analysis confirmed that animals demonstrating sustained human engraftment were homozygous for *Alb-uPA*, whereas the subset with failing graft function was hemizygous.

Murine livers are repopulated with human hepatocytes

Sections from transplanted homozygote livers showed large nodules of hepatocytes arranged in typical cord-like structures (Fig. 2*a*). Within nodules, hepatocyte cytoplasm and nuclei appeared histologically normal compared with surrounding tissues where cells were obviously smaller, with vacuolated cytoplasm and pyknotic nuclei (Fig. 2*b*). We immunostained sections with a monoclonal antibody that intensely stained control human liver but did not cross-react with non-transplanted homozygous mouse liver, either within or outside of endogenously produced regen-

Table 1 Infection of homozygous mice with human HCV

Alb-uPA genotype	*n*	Initial human-albumin signal	Median graft duration (wk)	HCV RNA (RT-PCR)
–/–	8	none[a]	0	0/8
+/–	15	strong	15.5	0/15
+/+	4	strong	30.5[b]	4/4[c]

Association between homozygosity of the *Alb-uPA* transgene and development of both sustained human chimerism and infection with human HCV. Graft duration defined as the period of human-albumin detectability by immunoprecipitation/western-blot procedure. [a], 3/8 animals had a single weak human-albumin signal at 5-wk timepoint only. [b], $P < 0.001$ versus hemizygotes and wild type by Kruskal–Wallis test. [c], $P < 0.001$ versus hemizygotes and wild type by Pearson χ^2 test.

erative nodules (Fig. 2*c*, *d* and *e*). This showed that the nodules were clearly of human origin, expanding outward into and compressing surrounding murine-derived tissues (Fig. 2*f* and *g*). Biliary tract and portal structures appeared to be mainly host-derived, as observed by Rhim *et al.*[10]

For additional confirmation of human chimerism, we isolated genomic DNA from livers of transplanted and nontransplanted mice, and we distinguished murine and human DNAs using a PCR-based strategy to detect *Alu* elements, which are short interspersed sequence elements found only in primate genomes[11] (Fig. 2*h*). *AluSx* is the most abundant subfamily and is thought to represent the general human *Alu* consensus. We confirmed the presence of murine genomic DNA by PCR amplification of a sequence mapping to the murine *c-mos* proto-oncogene[12]. As expected, nontransplanted mouse liver DNA and mouse-tail biopsy DNA contained the proto-oncogene but no *Alu*-repeats, whereas human peripheral blood contained *Alu*-repeats but not the proto-oncogene. Analysis of DNA extracted from a transplanted mouse liver clearly showed both bands, establishing the presence of human genomic DNA within the liver.

Establishment of HCV infection in transplanted mice

With evidence of prolonged human engraftment, we next infected mice with serum from HCV-infected human donors. We transplanted non-infected human hepatocytes into 27 offspring from heterozygous crosses, and at 6 weeks after transplantation all mice were inoculated intravenously and/or intraperitoneally with 0.25 ml human serum obtained from 1 of 2 unrelated HCV-positive donors (viral genotypes 1a and 6a). We analyzed selected serum samples between 3 and 40 weeks after inoculation for the presence of positive-strand HCV RNA by reverse transcriptase (RT)-PCR (Table 1).

All eight wild-type controls showed no initial graft function and were persistently negative for HCV RNA. Hemizygous animals had initially strong human-albumin signals, but gradually showed diminishing signal intensity to a median graft duration of 15.5 weeks; we could not detect positive-strand HCV RNA in any of these animals over multiple time points. In sharp contrast, all four animals homozygous for the *Alb-uPA* transgene demonstrated sustained human chimerism (median, 30.5 wk) and were positive for HCV RNA as shown by RT-PCR analysis of serum. Quantitative HCV RNA analysis revealed that viral levels, ranging from 1.4×10^3 to 1.4×10^6 RNA copies/ml, were well within the range of infected humans. Successful infections were established with both genotypes of viral inoculum, and duration of infection ranged from 10 to 21 weeks in this initial cohort.

HCV infection is dependent on *Alb-uPA* homozygosity

Whereas positive-strand HCV RNA was persistently demonstrable in homozygous mice, we were unable to detect it in hemizygotes. We hypothesized that hemizygotes fail to support HCV replication at detectable levels after diminished initial engraftment and earlier graft loss. We developed a protein dot-blot assay using chemiluminescence and phosphoimaging to more accurately quantify human albumin production. After transplanting 1×10^6 cryopreserved human hepatocytes from a single human donor into 21 recipients (15 homozygotes and 6 hemizygotes), we sampled randomly selected animals for quantitative human-albumin analysis and/or immunohistochemical analysis.

Whereas hemizygous and homozygous animals initially showed similar human-albumin signal intensities, by 5–6 weeks a clear divergence was apparent and by 10–12 weeks human-albumin signals in homozygous mice were more than an order of magnitude higher than hemizygotes (Fig. 3*a*). To estimate the percent replacement of murine liver with human tissue, random liver sections from recipients killed at selected time points after transplantation were immunostained with a monoclonal antibody specific for hepatocytes. These immunohistochemical data confirmed the protein dot-blot findings, with human cells occupying substantial portions (≥ 50%) of cross-sectional liver area in homozygous mice (Fig. 3*b*). In distinct contrast, we examined multiple sections of tissue from heterozygous recipients, and found only minimal evidence of human engraftment (Fig. 3*c*).

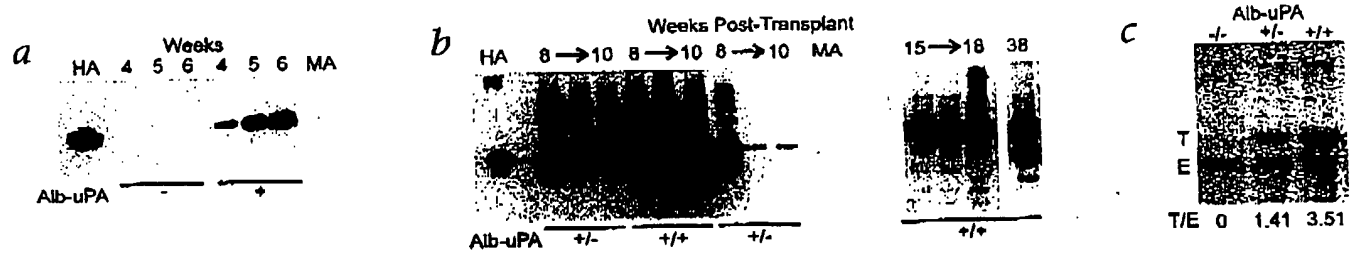

Fig. 1 Detection of human albumin (HA) produced from human hepatocytes in chimeric livers (samples represent individual mice). *a*, Western-blot analysis showing early HA production in wild-type (–) or transgenic (+) recipients; incremental rise in HA signal indicates graft expansion. *b*, Western-blot analysis showing long-term HA production in transplant recipients hemizygous (+/–) or homozygous (+/+) for the *Alb-uPA* transgene. Blot demonstrates diminishing signal in hemizygotes, contrasted with persisting signal in homozygotes. HA in leftmost lane, HA standard; MA in rightmost, nontransplanted mouse serum (negative control). *c*, Southern-blot analysis for determination of *Alb-uPA* zygosity from genomic DNA. A transgenic uPA:endogenous nuPA (T/E) ratio of ~2 is characteristic of hemizygous mice, whereas homozygotes have a ratio of ~4.

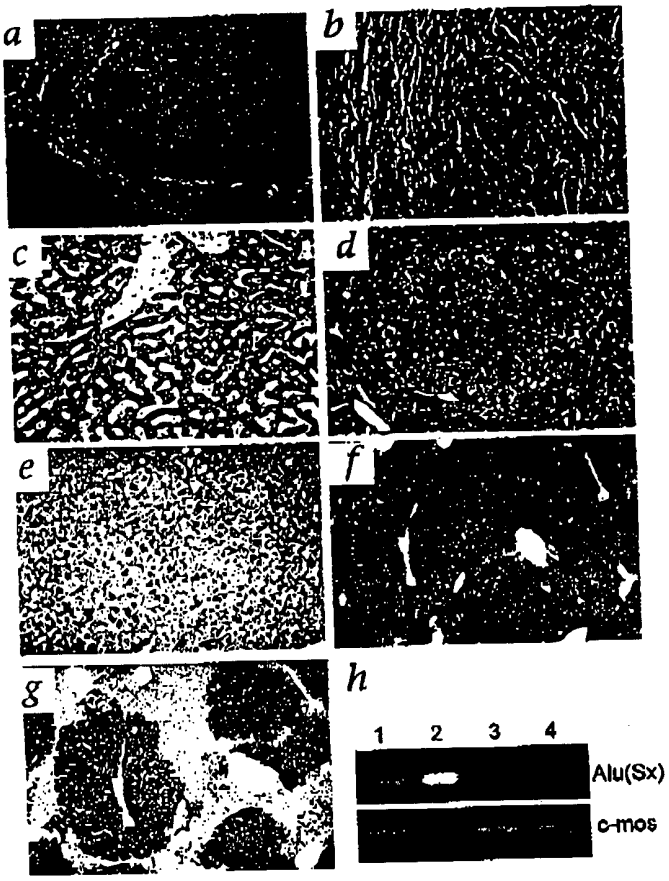

Fig. 2 Histochemical analysis of human chimerism in mouse livers. *a* and *b*, Transplanted homozygote stained with H&E. *c*, Human liver immunostained with monoclonal antibody against human hepatocytes. *d*, Nontransplanted homozygote with mouse-derived regenerative nodule; H&E stained. *e*, Serial section from *d* immunostained as in *c*. *f*, Transplanted homozygote stained with H&E. *g*, Serial section from *f* immunostained with monoclonal antibody against human hepatocytes. Magnifications, ×40 (*a*, *f*, and *g*) and ×200 (*b*, *c*, *d* and *e*). *h*, Genomic DNA extracted from liver of a transplanted homozygous *Alb/uPA* mouse and analyzed for human-specific *AluSx* consensus sequence or murine-specific *c-mos* proto-oncogene. *AluSx* consensus was detected in genomic DNA from transplanted *Alb/uPA* murine liver (lane 1) and human peripheral blood (lane 2) but not from non-transplanted control *Alb/uPA* murine liver (lane 3) or murine control tails (lane 4).

Together, these studies indicate a substantial advantage in both the magnitude and duration of human hepatocyte engraftment for homozygous *Alb-uPA* recipients compared with their heterozygous counterparts.

By transplanting into the progeny of heterozygous crosses, we established successful infections in 4/27 mice, all homozygotes. This success rate would make the model too cumbersome for routine use. As a result of the quantitative advantage in graft size ascribed to homozygous mice, we shifted our breeding colony towards exclusive production of homozygous *Alb-uPA* mice. Using our dot-blot assay to screen early for high-level hepatocyte engraftment (human-albumin levels > 250μg/ml), approximately 75% of HCV-inoculated animals developed persistent viral titers of more than 3×10^4 copies/ml, with as many as 1×10^6 copies/ml. The rest of our viral studies were therefore performed in homozygous recipients.

Long-term persistence of HCV infection

Persistence of viral titers in humans is the result of ongoing active proliferation. However, in immunocompromised chimeric animals, it is possible that HCV persistence is due to slower viral elimination rather than true infection and replication. Five homozygous graft recipients were inoculated with 250 μl infected human serum (genotype 3a; 2.95×10^6 viral RNA copies/ml); each animal therefore received an inoculum of 7.38×10^5 RNA copies. In 3/5 recipients, viral titers increased by 16-, 27- and 36-fold, respectively, over the initial inoculum by 5 weeks after inoculation (Fig. 3*d*). In the remaining 2 recipients, titers increased modestly over 5 weeks (1.6- and 4.3-fold, respectively). In this cohort of mice, detection of positive-strand HCV RNA was confirmed at 15 weeks after inoculation in 1 animal and at 17 weeks in 2 others (one early death after blood sampling). In the fifth mouse, productive infection with HCV was ongoing at 35 weeks after inoculation with viral titers of 1.67×10^5 copies/ml. The initial rise in titers coupled with persistently high viral levels at 35 weeks is consistent with viral replication, and cannot be ascribed to carryover artifact.

A 3-log rise in viral titers after inoculation with HCV

To detect an initial rise in viral titers that might be masked by a

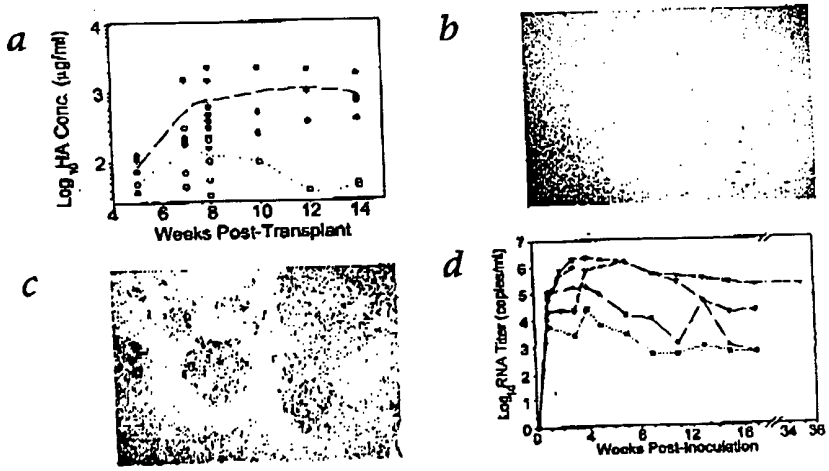

Fig. 3 Mice homozygous for the *Alb-uPA* transgene support quantitatively higher levels of human hepatocyte engraftment than hemizygotes. *a*, Vertica-scatter plot of quantified HA production from individual homozygous (●) or hemizygous (○) recipient mouse serum samples. Median trend lines are shown for both groups. *b* and *c*, Photos show representative sections taken from heterozygous (*b*) and homozygous (*c*) *Alb-uPA* graft recipients at 12 wk after transplantation immunostained with anti-human hepatocyte antibodies. *d*, Rising serum HCV RNA titers over time in homozygous transgenic graft recipients after inoculation with HCV-infected human serum. Each different line and symbol represents serial titers from an individual graft recipient.

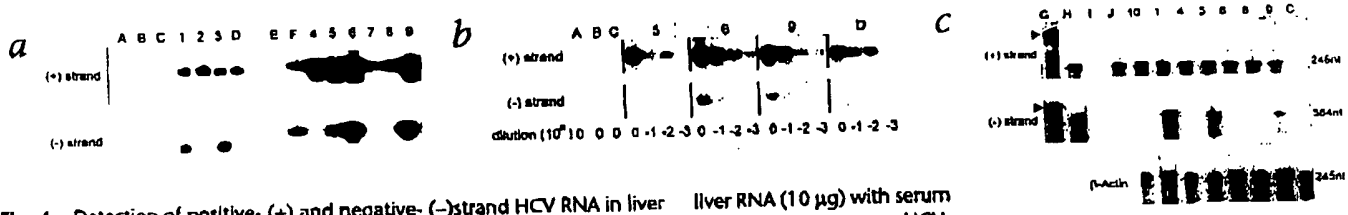

Fig. 4 Detection of positive- (+) and negative- (–)strand HCV RNA in liver samples taken from infected homozygous chimeric mice. Letter designations ('A' through 'J', specified below and consistent through the figure) represent different RNA control samples, and number designations (1 through 10, specified below and consistent through the figure) represent individual RNA samples isolated from the livers of 10 homozygous mice that were transplanted and then inoculated with HCV-infected human serum. *a*, Detection of (+)strand RNA (upper) or (–)strand RNA (lower) by thermostable rTth reverse transcriptase RNA PCR protocol with strand-specific primers. Lanes: A, wild-type control mouse, nontransplanted, noninfected; B, heterozygous transplanted mouse inoculated with HCV; C, homozygous transplanted mouse not inoculated with HCV; D, infected human serum; E, standard DNA ladder; F, binding of labeled probe to target DNA sequences generated from (+)strand (upper) or (–)strand (lower) viral RNA; G, mouse liver RNA (10 μg) with serum added RNA from an HCV-positive human; H, mouse liver RNA (10 μg) added with 1×10^6 copies radioinert antisense (upper) or sense (lower) riboprobe; I, mouse liver RNA (10 μg) added with 1×10^6 copies radio-inert sense (upper) or antisense (lower) riboprobe; J, riboprobes hybridized with 10 μg mouse liver RNA, all subsequent steps identical except addition of RNase. *b*, Dilution-series analysis of selected animals using thermostable rTth reverse transcriptase RNA PCR protocol. *c*, Detection of (+)strand HCV RNA (upper), (–)strand HCV RNA (middle) or β-actin RNA (lower) by RNase protection assay. Fragments in lane G represent undigested riboprobe (arrowhead), with expected lengths greater than those of corresponding fragments protected by hybridization to their targets. Control lanes are as designated above; mouse 10 was analyzed only by the RPA method.

higher viral inoculum, we infected a sixth chimeric mouse with a much smaller viral inoculum (1.35×10^3 RNA copies), and then followed at weekly intervals. This mouse rapidly developed HCV infection, and the total serum viral load at 10 weeks after infection was measured at 1.33×10^6 copies, a 1000-fold increase. In 2 subsequent animals inoculated with 1.05×10^5 copies and 1.75×10^3 copies, titers rose to 9.5×10^5 copies/mL at 10 weeks and 3.42×10^6 copies/mL, respectively, at 5 weeks post-inoculation; rises of 905-fold and 1954-fold, which confirm the initial 10-week result. A nonproductive interaction could not reasonably sustain a 3-log increase in viral load, strongly supporting the occurrence of viral replication.

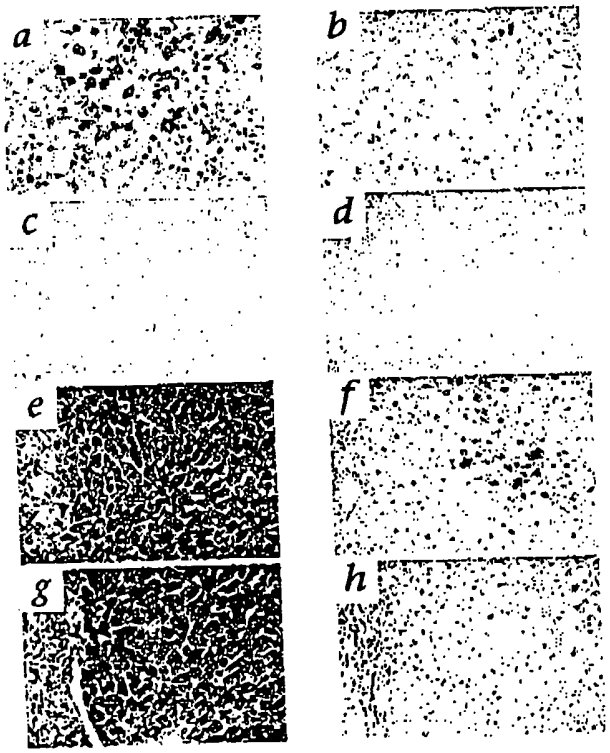

Negative-strand viral RNA in recipient livers

HCV is a positive-strand RNA virus replicating through a negative-strand intermediate; detection of negative-strand HCV RNA within the liver constitutes proof of replication. This replicative intermediate is believed to exist at levels 10–100 times lower than its positive-strand template[13,14], and hence its detection can be more difficult.

Nine homozygous graft recipients inoculated with 5×10^5 copies of viral RNA from freshly obtained human serum showed positive-strand HCV RNA at 3–4 weeks post-inoculation (Fig. 4*a*, upper). Samples of liver tissue were obtained by 50% partial hepatectomy at 2–5 weeks post-inoculation in 7 mice and 12–13 weeks in the remaining 2 mice. Analysis for negative-strand HCV RNA was performed in blinded fashion by an independent laboratory (A.R.) using a thermostable rTth RT-RNA PCR (rTth PCR) protocol and strand-specific primers (Fig. 4*a*, lower panel). In 5/9 samples analyzed, negative-strand RNA was detected; the 2 samples taken at 12–13 weeks post-inoculation did not show negative-strand RNA. To reduce the risk of false-positive results[15], we performed two additional sets of confirmatory experiments.

Using rTth PCR, we performed a dilution series on three animals to confirm dilutability of the negative-strand signal (Fig. 4*b*). Positive-strand signal was detectable over 3-log dilutions in 2/3 animals as well as control human serum. As expected, no negative-strand signal was detected in human serum. In 2/3 mice, the negative-strand signal was clearly detectable after 10-fold dilution. In the third mouse, we did not detect the negative-strand; the diminished positive-strand signal for this animal

Fig. 5 Immunohistochemical detection of HCV proteins within human hepatocytes in transplanted homozygous *Alb-uPA* mice. *a* and *b*, Serial sections of HCV-infected human liver stained for HCV with monoclonal antibody against NS3/NS4 (TORDJI-21) (*a*) or by an unrelated isotype-specific monoclonal antibody against melanoma (HMB-45) (*b*). *c* and *d*, Serial sections from non-infected human liver stained with TORDJI-21 (*c*) or HMB-45 (*d*). *e* and *f*, Serial sections from a transplanted homozygous mouse infected with HCV, stained with antibody against human hepatocytes (*e*) and HCV-specific antibody (TORDJI-21) (*f*). Arrows indicate coarse granules specific for HCV infection. *g* and *h*, Serial sections from a control noninfected homozygous mouse transplanted with human hepatocytes and stained with anti-human hepatocyte antibody (*g*) or TORDJI 21 (*h*).

indicates comparatively less RNA was loaded onto these lanes of the gel. Lack of additional sample material prevented repeat analysis by this method; however, we subsequently confirmed the presence of the negative-strand using the RNase protection method.

In a further confirmatory experiment, we assayed six animals previously tested by the above PCR method (plus one additional animal) for negative-strand RNA using an RNase protection assay developed in our laboratory (Fig. 4*c*). Results from this system were concordant with the previous PCR findings in 5/6 mice, confirming presence of negative-strand RNA in 3/4 mice and absence in the remaining 2 mice, which initially tested negative by rTth PCR. We were unable to confirm presence of the negative-strand in one mouse; this variance might be attributable to the less sensitive nature of the RNase-protection assay.

These separate and independently performed assays clearly demonstrate presence of negative-strand HCV RNA within chimeric livers sampled at 2–5 weeks post-inoculation. Our previous experiments with sequential weekly analysis by quantitative RT-PCR demonstrated a rapid rise in HCV serum titer at weeks 2–4 after inoculation, corresponding to maximal rates of viral replication within the liver. We would expect this to be paralleled by maximal amounts of negative-strand viral RNA. After this period of rapid replication, viral levels stabilize, indicating that although ongoing replication clearly occurs, the rate diminishes to equal that of viral loss. This might explain why negative-strand RNA is detectable earlier in infections (5/6 animals sampled at 2–5 wk) rather than later (0/2 sampled at 12–13 wk). Together, these data conclusively support active viral replication in this mouse model.

HCV infection can be serially passaged

We intraperitoneally injected fresh serum from a human donor (250 µl; 4.75×10^5 viral RNA copies) into a naive chimeric mouse; at four weeks after inoculation, viral titers were 1.76×10^6 copies/ml. Serum taken from this mouse (125 µl; ~2.19×10^5 RNA copies) was injected intraperitoneally into a second naive chimeric mouse, which developed titers of 1.75×10^4 copies/ml at four weeks after inoculation. Serum from this first-passage recipient was then injected (100 µl; ~1.75×10^3 RNA copies) into a third naive chimeric mouse. At five weeks after inoculation, this second-passage recipient had viral titers of 3.42×10^5 copies/ml. Serum from this second-passage recipient (20 µl) was injected into two additional naive mice (third-passage recipients), both of whom subsequently developed HCV infections with viral titers of 1.6×10^5 and 4.5×10^6 at 9 and 11 weeks post-inoculation, respectively. If one assumes the null hypothesis that replication does not occur but rather the initial human inoculum persists, these third-passage recipients would have received approximately 120 copies of virus from the initial inoculum (4.75×10^5 viral copies × 1:8 dilution × 1:10 dilution × 1:50 dilution, assuming mouse serum volume ~1000 µl). At 27 weeks after the initial inoculation from human to mouse, these third-passage recipients had up to 37,500-fold more measured viral RNA than would have been received from the original human inoculum. We have replicated this experiment through two passages in two other series of mice, and through a single passage in a third leading to amplification of viral RNA from 90- to 1057-fold over the initial human inoculum. This transmission from human → mouse → mouse → mouse → mouse represents both replication of the HCV genome and production of fully infectious particles.

HCV infects human hepatocytes in transplant recipients

To colocalize HCV infection in human hepatocytes within the livers of chimeric mice, we immunostained sections of liver taken from homozygous transplanted mice with productive HCV infections with a monoclonal antibody against the NS3/NS4 portion of the viral polyprotein. Control sections of infected human liver showed staining localized to hepatocytes, with sparing of both portal triad structures and areas of bridging fibrosis (Fig. 5*a*). Using the rigorous immunohistochemical criteria defined by Brody *et al.*[16], infected cells are characterized by coarse intracytoplasmic granules (Fig. 5*a*, arrows); the diffuse fine granular cytoplasmic staining seen in sections is considered nonspecific. An unrelated isotype-specific control antibody produced no staining within hepatocytes, and sections taken from a noninfected human liver showed no staining with either antibody (Fig. 5*b–d*). Serial sections taken from the liver of a transplanted mouse with a productive HCV infection clearly show characteristic coarse cytoplasmic granules localized within nodules of human hepatocytes, with slightly diminished intensity compared with human controls (Fig. 5*e* and *f*). We detected HCV antigens only in human hepatocytes, with no staining in the surrounding hepatocytes of murine origin. Although human cells are clearly present in transplanted homozygous mice not infected with HCV, HCV antigens are not present (Fig. 5*g* and *h*). This immunohistochemical data provides convincing evidence that HCV infects human hepatocyte nodules within chimeric livers of transplanted *Alb-uPA* mice.

Discussion

These experiments establish that homozygous SCID/*Alb-uPA* mice with chimeric human livers can be infected *de novo* with HCV-positive human serum; they support HCV replication within the human portion of their livers at clinically relevant titers; and they show the capacity to transmit this infection to other chimeric mice. Successful infections were established with viral genotypes 1a, 1b, 3a and 6a, with rapid increases in viral RNA titers to levels easily detected by standard commercial assays. We successfully established infections in chimeric mice 3–8 weeks after transplantation, and did most of our inoculations between 4–6 weeks post-transplant, subject to the availability of infected human serum.

Homozygosity of *Alb-uPA* is critical to successful establishment of viral infection, and by using homozygotes as recipients, coupled with early screening of graft function by dot-blot analysis, HCV infections are routinely established in approximately 75% of all inoculated mice. Earlier reports suggested prohibitively high perinatal mortality rates associated with homozygosity of the *Alb-uPA* transgene. Since inception of our homozygous Alb-uPA colony, we have experienced a perinatal mortality rate of 32.6%, which is slowly decreasing with improvements in breeding stock. Using 8 breeding females and 4 breeding males provides ample potential recipient mice available at the ideal recipient age of 5–14 days at any one time.

The transplantation procedure requires basic microsurgical equipment and technical skills and takes 5–6 minutes per animal. While access to human hepatocytes might be limiting for some investigators, the yields from hepatocyte isolations in our laboratory average $2–3 \times 10^8$ viable human cells, similar to that of others[17,18]. Given the 9–10 day window optimal for transplantation and modest collaboration between investigators and hepatobiliary surgeons to use surplus tissue, fresh hepatocytes can almost always be available for transplantation—we have almost

no unused mice in our colony. The ability to cryopreserve surplus cells might allow for transportation to centers without human tissue access, although our experience with cryopreserved cells is considerably more limited; we have had success in both establishing long-term grafts (albeit at a lower overall success rate) and producing HCV infections within these animals.

This model should allow investigators to begin directly exploring *in vivo* strategies for inhibiting viral replication or preventing infection by passive immunity, and it should significantly advance the search for new antiviral therapies and vaccine development for hepatitis C.

Methods

Development of SCID/*Alb-uPA* strain. Animals were housed VAF, following Canadian Council on Animal Care (1993) guidelines. Experimental approval came from the University of Alberta Animal Welfare Committee. Hemizygous *Alb-uPA* mice (strain TgN(*Alb1Plau*)144Bri, Jackson, Bar Harbor, Maine) were crossed with homozygous SCID/*bg* mice (strain C.b-17/GbmsTac-SCID/*bg*N7, Taconic Farms, Germantown, New York). *Alb-uPA* was amplified from genomic DNA by PCR (Jackson). Homozygosity of the SCID trait was confirmed by quantification of total serum IgG using a sandwich ELISA.

Isolation of human hepatocytes. Ethical approval was obtained from the University of Alberta Faculty of Medicine Research Ethics Board and informed consent from all hepatocyte donors. Segments of human liver tissue (15–20 cm^3) were obtained from resection specimens normally discarded; most operations were performed for intrahepatic malignancies. After rapid cooling, hepatocytes were isolated and purified by collagenase-based perfusion[19,20], using 0.38 mg/ml Liberase CI (Boeringer) in perfusate, and stored short-term in 0°C Belzer-UW solution (DuPont, Wilmington, Delaware). Cell counts (hemocytometer) and viability (Trypan blue) were confirmed before use; viability was routinely > 80%.

Cryopreservation and thawing of human hepatocytes. Isolated hepatocytes were suspended (1×10^7 hepatocytes/ml) in cryopreservation tubes in 4 °C freeze/thaw media (50 ml FCS, 2.5 ml Pen/Strep, 447.5 ml M199 media). On ice, 2M DMSO was added in aliquots of 0.5 ml, 2 ml and 4 ml at 0, 5 and 30 min, respectively. At 45 min, tubes were transferred to a programmable ethanol freezing bath pre-set at –7.4 °C, 'nucleated' with a liquid-N_2-cooled semiconducting rod, cooled at 1 °C/min to –40 °C, and stored indefinitely in liquid N_2. Cells were rapidly reheated to 0 °C in a 37 °C water bath and spun, and supernatant was discarded. On ice, 1 ml of 0.75M sucrose was added at 0 min. Freeze/thaw media was serially added (1, 1, 2 and 4 ml at 30, 35, 40 and 45 min). At 50 min, the supernatant was separated, and cells were resuspended in Belzer-UW solution (Dupont) at 0 °C.

Transplantation of human hepatocytes. Recipients (5–14-day-old) were anesthetized with halothane/O_2, and through a small left-flank incision, 1×10^6 viable hepatocytes were injected into the inferior splenic pole; a single titanium clip was placed across the injection site for hemostasis, and the incision was closed.

Detection of human albumin in mouse serum by immunoprecipitation and western-blot analysis. Mouse serum (20 µl) was incubated with monoclonal antibody against human albumin (Clone HSA-9; Sigma) and complexes collected with protein G-agarose beads (Boehringer). Under reducing conditions, immunoprecipitates were separated by SDS–PAGE and transferred to nitrocellulose. Western blots were prepared using a biotinylated monoclonal antibody against human albumin (Clone HSA-11, Sigma), with a streptavidin-HRP conjugate and chemiluminescent substrate (Pierce, Rockford, Illinois) for detection.

Determination of zygosity of the *Alb-uPA* transgene. Mouse DNA (3 µg) was digested with PvuII, size fractionated on 0.7% agarose gel, transferred to Hybond-N+ membrane (Amersham), and hybridized to a ^{32}P-labeled probe from the final intron of the *uPA* gene (positions 7312–7920, GenBank accession #M17922). A 2.88-kb band was derived from *uPA* transgenes (T) and a 2.53-kb band from endogenous *uPA* genes (E); hybridization was quantified with a Fuji phosphoimager and Image Gauge Software (Fujifilm, Stamford, Connecticut).

Immunohistochemistry. Mouse liver biopsies fixed in 10% formalin were paraffin embedded. Sections (5 µm) were H&E stained in standard fashion. To detect human hepatocytes, sections pre-treated with an avidin/biotin blocking kit (Zymed Laboratories, San Francisco, California) were immunostained with a monoclonal antibody against human hepatocyte (Clone OCH1E5, 1:20 dilution; DAKO, Carpinteria, California), with bound antibody detected by Super Sensitive Immunodetection System (BioGenex, San Francisco, California). For HCV proteins, sections were immunostained with monoclonal antibody against NS3/NS4 (TORDJI-22; Biogenex)[16]; isotype-specific unrelated monoclonal antibody against human melanoma (Clone HMB 45; Enzo Diagnostics, Farmingdale, New York) was used as a control.

Protein dot-blot assay for quantification of human-albumin production. Samples of mouse serum (2 µl) incubated for 5 min at 100 °C in 40 µl reducing buffer were triplicate blotted onto nitrocellulose. Dried membranes were soaked in transfer buffer, blocked with 3% PBS-Tween, and prepared as western blots. Chemiluminescence was quantified (STORM phosphoimager) from standard curves on each blot.

Detection of human DNA within transplanted mouse liver. Genomic DNA was isolated by phenol-chloroform, and *Alu* repeats amplified by PCR using *Alu Sx*-specific primers R16A/6 (5'-GGCGCGGTGGCTCACG-3') and L23A/266 (5'-TTTTTTGAGACGGAGTCTCGCTC-3')[21]. Human peripheral blood served as a positive control and *Alb/uPA* tails and non-transplanted *Alb/uPA* liver as negative controls. Murine genomic DNA was detected by amplifying a sequence from the murine *c-mos* proto-oncogene, using MUSMOS A (5'-GAATTCAGATTTGTGCATACACAGTGACT-3') and MUSMOS B (5'-AACATTTTTCGGGAATAAAAGTTGAGT-3').

Quantitative analysis of positive-strand HCV RNA in mouse serum. Blinded analysis was performed by the Alberta Provincial Laboratory of Public Health (Edmonton, Canada), or the Canadian Center for Disease Control (Winnipeg, Canada), using the Cobas Amplicor HCV Monitor system (Roche Diagnostics, Laval, Canada).

Detection of negative-strand HCV RNA by rTth PCR. Total RNA was isolated from mouse liver biopsies or infected human serum using TRIZOL (GIBCO/BRL, Burlington, Canada). RT-PCR was performed using a thermostable rTth reverse transcriptase RNA PCR kit (Perkin-Elmer, Norwalk, Connecticut). Positive-strand RNA was detected with an antisense (5'-CTCGCAAGCCCCTATCAGG-3') primer and negative-strand with a sense (5'-GAAAGCGTCTAGCCATGGCGT-3') primer for reverse transcription[22]. Strand-specific cDNA was amplified by adding the other primer to target a 240-bp region of the 5' non-coding region, using 35 cycles at 95 °C for 30 s, 66 °C for 45 s and 70 °C for 90 s, followed by 70 °C for 5 min. Reaction products were loaded onto a 2% agarose gel, transferred to Hybond-N+ nylon membrane (Amersham) and hybridized with an α-^{32}P-labeled DNA probe for HCV 5' non-coding region at 42 °C overnight.

Detection of negative-strand HCV RNA by RNase protection assay. Total RNA was isolated from mouse liver using Trizol Reagent (GIBCO/BRL) and from HCV-infected human serum using QIAamp Viral RNA Mini Kit (Qiagen, Valencia, California). Extracted RNA was probed with ^{32}P-labeled, gel-purified antisense riboprobe (detection of positive strand), sense riboprobe (detection of negative strand) and/or β-actin antisense riboprobe. Details of plasmid synthesis and riboprobe construction are available (Methods, Web Supplement). Denatured RNA samples were hybridized overnight at 42 °C, and RNase digestion was performed using an RNase protection assay kit (Ambion RPA III Kit, Austin, Texas). Products were resolved on a 5% PAGE containing 8 M urea and exposed to Kodak X-Omat AR film (Kodak, Vancouver, Canada).

Note: Supplementary information is available on the Nature Medicine website (http://medicine.nature.com/supplementary_info/).

Acknowledgments

We thank C.A. Compston for invaluable assistance with the RPA assay; T. Covanagh for providing enzymes; M. Craig for assistance with western-blot analysis; and P. Dickie for assistance with genotyping offspring.

RECEIVED 18 DECEMBER 2000; ACCEPTED 15 JUNE 2001

1. Sarbah, S. & Younossi, Z. Hepatitis C: An update on the silent epidemic. *J. Clin. Gastro.* 30, 125–143 (2000).
2. Choo, Q.L. *et al.* Isolation of a cDNA clone derived from a blood borne non-A non-B viral hepatitis genome. *Science* 244, 359–361 (1989).
3. Heckel, J., Sandgren, E., Degen, J., Palmiter, R. & Brinster, R. Neonatal bleeding in transgenic mice expressing urokinase-type plasminogen activator. *Cell* 62, 447–456 (1990).
4. Sandgren, E. *et al.* Complete hepatic regeneration after somatic deletion of an albumin-plasminogen activator transgene. *Cell* 66, 245–256 (1991).
5. Rhim, J., Sandgren, E., Degen, J., Palmiter, R. & Brinster, R. Replacement of diseased mouse liver by hepatic cell transplantation. *Science* 263, 1149–1152 (1994).
6. Petersen, J., Dandri, M., Gupta, S. & Rogler, C. Liver repopulation with xenogeneic hepatocytes in B and T cell-deficient mice leads to chronic hepadnavirus infection and clonal growth of hepatocellular carcinoma. *Proc. Natl. Acad. Sci. USA* 95, 310–315 (1998).
7. Brown, J. *et al.* A long-term hepatitis B viremia model generated by transplanting nontumorigenic immortalized human hepatocytes in Rag-2 deficient mice. *Hepatology* 31, 173–181 (2000).
8. Petersen, J. *et al.* Hepatocytes isolated from the adult human liver can repopulate the liver of uPA/Rag-2 mice and support hepatitis B virus infection and replication. *Hepatology* 30, 423A (1999).
9. Clement, B. *et al.* Long-term co-cultures of adult human hepatocytes with rat liver epithelial cells: Modulation of albumin secretion and accumulation of extracellular material. *Hepatology* 4, 373–380 (1984).
10. Rhim, J., Sandgren, E., Palmiter, R. & Brinster, R. Complete reconstitution of mouse liver with xenogeneic hepatocytes. *Proc. Natl. Acad. Sci. USA* 92, 4942–4946 (1995).
11. Schmid, C.W. *Alu*: Structure, origin, evolution, significance, and function of one-tenth of human DNA. *Prog. Nucl. Acid Res. Mol. Biol.* 53, 283–319 (1996).
12. Van Beveren, C., van Straaten, F., Galleshaw, J. & Verma, I. Nucleotide sequence of the genome of a murine sarcoma virus. *Cell* 27, 97–108 (1981).
13. Mellor, J., Haydon, G., Blair, C., Livingstone, W. & Simmonds, P. Low level or absent *in vivo* replication of hepatitis C virus and hepatitis G virus/GB virus C in peripheral blood mononuclear cells. *J. Gen. Virol.* 79, 705–714 (1998).
14. Lanford, R., Chavez, D., Chisari, F.W. & Sureau C. Lack of detection of negative-strand hepatitis C virus RNA in peripheral blood mononuclear cells and other extra-hepatic tissues by the highly-specific rTth reverse transcriptase PCR. *J. Virol.* 69, 8079–8083 (1995).
15. Lanford, R., Sureau, C., Jacob, J., White, R. & Fuerst, T. Demonstration of *in vitro* infection of chimpanzee hepatocytes with hepatitis C virus using strand-specific RT/PCR. *Virology* 202, 606–614 (1994).
16. Brody, R. *et al.* Immunohistochemical detection of hepatitis C antigen by monoclonal antibody TORDJI-22 compared with PCR viral detection. *Am. J. Clin. Path.* 110, 32–37 (1998).
17. Ballet, F. *et al.* Isolation, culture and characterization of adult human hepatocytes from surgical liver biopsies. *Hepatology* 4, 849–854 (1984).
18. Dorko, K. *et al.* A new technique for isolating and culturing human hepatocytes from whole or split livers not used for transplantation. *Cell Transplant.* 3, 387–395 (1994).
19. Seglen, P. Preparation of isolated rat liver cells *Meth. Cell. Biol.* 13, 29–83 (1976).
20. Ryan, C., Carter, E., Jenkins, R. & Sterling, L. Isolation and long-term culture of human hepatocytes. *Surgery* 113, 48–54 (1993).
21. Zietkiewicz, E., Labuda, M., Sinnett, D., Glorieux, G. & Labuda, D. Linkage mapping by simultaneous screening of multiple polymorphic loci using *Alu* oligonucleotide-directed PCR. *Proc. Natl. Acad. Sci. USA* 89, 8448–8451 (1997).
22. Murphy, D., Willems, B. & Delage, G. Use of the 5′ noncoding region for genotyping hepatitis C virus. *J. Inf. Dis.* 169, 473–475 (1994).